Mathematical modeling elucidates the role of transcriptional feedback in gibberellin signaling

Alistair M. Middleton[a,b,c], Susana Úbeda-Tomás[a], Jayne Griffiths[d], Tara Holman[a], Peter Hedden[d], Stephen G. Thomas[d], Andrew L. Phillips[d], Michael J. Holdsworth[a], Malcolm J. Bennett[a], John R. King[a,c], and Markus R. Owen[a,c,1]

[a]Centre for Plant Integrative Biology, School of Biosciences, University of Nottingham, Loughborough LE12 5RD, United Kingdom; [b]Zentrum für Biosystemanalyse, Albert-Ludwigs-Universität, 79104 Freiburg im Breisgau, Germany; [c]Centre for Mathematical Medicine and Biology, School of Mathematical Sciences, University of Nottingham, Nottingham NG7 2RD, United Kingdom; and [d]Plant Science Department, Rothamsted Research, Harpenden, Herts AL5 2JQ, United Kingdom

Edited by Mark Estelle, University of California at San Diego, La Jolla, CA, and approved March 8, 2012 (received for review August 24, 2011)

The hormone gibberellin (GA) is a key regulator of plant growth. Many of the components of the gibberellin signal transduction [e.g., GIBBERELLIN INSENSITIVE DWARF 1 (GID1) and DELLA], biosynthesis [e.g., GA 20-oxidase (GA20ox) and GA3ox], and deactivation pathways have been identified. Gibberellin binds its receptor, GID1, to form a complex that mediates the degradation of DELLA proteins. In this way, gibberellin relieves DELLA-dependent growth repression. However, gibberellin regulates expression of *GID1*, *GA20ox*, and *GA3ox*, and there is also evidence that it regulates *DELLA* expression. In this paper, we use integrated mathematical modeling and experiments to understand how these feedback loops interact to control gibberellin signaling. Model simulations are in good agreement with in vitro data on the signal transduction and biosynthesis pathways and in vivo data on the expression levels of gibberellin-responsive genes. We find that GA–GID1 interactions are characterized by two timescales (because of a lid on GID1 that can open and close slowly relative to GA–GID1 binding and dissociation). Furthermore, the model accurately predicts the response to exogenous gibberellin after a number of chemical and genetic perturbations. Finally, we investigate the role of the various feedback loops in gibberellin signaling. We find that regulation of *GA20ox* transcription plays a significant role in both modulating the level of endogenous gibberellin and generating overshoots after the removal of exogenous gibberellin. Moreover, although the contribution of other individual feedback loops seems relatively small, *GID1* and *DELLA* transcriptional regulation acts synergistically with *GA20ox* feedback.

Arabidopsis thaliana | plant hormone signaling

The plant hormone gibberellin (GA) acts as a key mediator between environmental cues and plant morphology in a variety of developmental processes, including stem and root elongation, seed germination, floral development, and determination of leaf size and shape (1). The gibberellin signal transduction and biosynthesis pathways have been genetically characterized in most detail in the model plants *Arabidopsis thaliana* (thale cress) and *Oryza sativa* (rice). In *Arabidopsis*, GA_4 (the main bioactive form) binds to one of its receptors [namely GIBBERELLIN INSENSITIVE DWARF (GID) 1a–c] (2, 3), causing a conformational change that enables the GA_4–GID1 complexes to bind DELLA proteins (4), which are subsequently tagged with ubiquitin for destruction by the 26S proteasome (5, 6) (Fig. 1, GA perception). DELLAs have been shown to suppress gibberellin-dependent growth processes (7–10).

The gibberellin biosynthesis pathway involves the conversion of the precursor, geranylgeranyldiphosphate, to bioactive GA_4 in a series of enzyme–substrate reactions (11). Regulation of gibberellin biosynthesis occurs mainly at the later stages of the pathway, for which the relevant enzymes are members of the GA 20-oxidase (GA20ox) and GA 3-oxidase (GA3ox) families that convert GA_{12} to GA_4 (Fig. 1, GA biosynthesis). Increasing the activity of enzymes that are earlier on the biosynthesis pathway does not significantly increase the GA_4 concentration (12). Gibberellins are deactivated by members of the GA2ox family (13–15), of which five members in *Arabidopsis* deactivate the bioactive C_{19} gibberellins (13).

Recent studies have identified genes that are responsive to gibberellin during seed germination (15, 16) and flowering (16). A subset of these genes have been shown to be direct targets of DELLAs (17) and will typically respond to gibberellin treatment within 15–30 min (as such, they are referred to as primary response genes). Some gibberellin primary response genes encode components of its signal transduction pathway (notably *GID1*) (2) and its biosynthesis pathway (through regulation of *GA20ox*, *GA3ox*, and *GA2ox* family members) (refs. 11 and 15 and references therein), indicating that a number of feedback loops modulate levels of gibberellin and how they are perceived in a cell.

In this work, we adopted a systems biology approach to studying gibberellin signaling in plant roots, although we expect that our observations will be relevant in other contexts. We generated root-specific transcriptomic data, identified the key gibberellin primary response genes to include in our mathematical model, and parameterized the model using our data and other published data. We validated the model using existing data and our data. We validated the model using additional experimental data, and finally, we probed the relative importance of the different feedback loops in the system.

Results and Discussion

Capturing Gibberellin Network Topology. The key gene families associated with gibberellin signaling are *GA2ox*, *GA3ox*, *GA20ox*, *DELLA*, and *GID1*. Their expression is typically localized to specific tissues, cell types, and developmental processes (18), and only a subset are subject to GA-regulated feedback (2, 13, 17, 19). Wild-type *Arabidopsis* roots have low sensitivity to the application of exogenous gibberellin, likely because of saturating levels of endogenous gibberellin (13). Therefore, gibberellin responses are typically investigated using mutant or transgenic plants that have low endogenous gibberellin (8). To obtain a clear understanding of which of the relevant genes are both expressed in roots and responsive to gibberellin, we generated transcriptomic data (*Materials and Methods*) from gibberellin-treated GA2ox1OE transgenic plant roots, which overexpress a *GA2ox* deactivation enzyme from runner bean *PcGA2ox1* (and therefore, have low endogenous gibberellin) (19).

Author contributions: A.M.M., S.Ú.-T., J.G., P.H., S.G.T., A.L.P., M.J.H., M.J.B., J.R.K., and M.R.O. designed research; A.M.M., S. Ú.-T., J.G., T.H., and M.R.O. performed research; A.M.M. and M.R.O. analyzed data; and A.M.M., S.Ú.-T., P.H., S.G.T., M.J.B., J.R.K., and M.R.O. wrote the paper.

The authors declare no conflict of interest.

This article is a PNAS Direct Submission.

Freely available online through the PNAS open access option.

[1]To whom correspondence should be addressed. E-mail: Markus.Owen@nottingham.ac.uk.

This article contains supporting information online at www.pnas.org/lookup/suppl/doi:10.1073/pnas.1113666109/-/DCSupplemental.

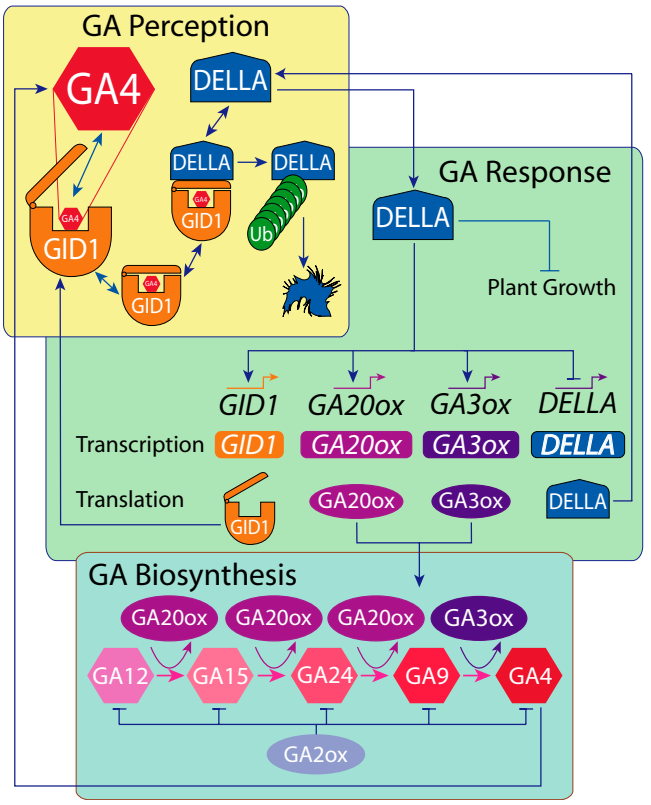

Fig. 1. The gibberellin signaling network is composed of three modules. Perception: gibberellin (GA_4) binds to the GID1 receptor, and this complex binds to DELLA proteins. The GA_4–GID1 complex then mediates the ubiquitination (indicated by Ub) of the DELLA proteins. Response: DELLA proteins mediate transcriptional activation of the *GID1*, *GA20ox*, and *GA3ox* genes and the repression of *DELLA* transcription. Biosynthesis: the enzyme GA20ox converts GA_{12} to GA_{15}, then to GA_{24}, and finally, to GA_9, which is subsequently converted to GA_4 by the enzyme GA3ox. Thus, activation of this pathway stimulates formation of GA_4 (provided that sufficient GA_{12} is available).

These findings complement published data from *ga1–3* plants (2, 17, 19) (Fig. 2*A*), which are also gibberellin-deficient because of a mutation in a biosynthesis enzyme upstream of GA_{12} (11). Consistent with the higher DELLA protein concentration to be expected in gibberellin-deficient plants, both *ga1–3* and GA2ox1OE have significantly shorter roots than WT, but this phenotype can be rescued by treating the plants with exogenous GA_4.

We found that only *GA20ox2*, *GA3ox1*, and *GID1a* (whose regulation by gibberellin has been described in refs. 2, 17, and 19) are expressed at significant levels and down-regulated by GA_4 treatment (Fig. 2*A*). Of the five *DELLA* family members in *Arabidopsis*, *GIBBERELLIC ACID INSENSITIVE* (*GAI*) and *REPRESSOR OF GA1-3* (*RGA*) have a role in regulating root elongation (8), and there is some evidence that they are up-regulated in seedlings in response to GA_3 (20). In rice shoots, *OsRGA* is up-regulated within 6 h, which is also in response to GA_3 (21). Our data indicate that *RGA* and *GAI* are up-regulated in *Arabidopsis* roots in response to GA_4 treatment (Fig. 2*A* and *SI Appendix*, Fig. S3). In contrast to their mRNAs, RGA and GAI protein concentrations will decrease because of gibberellin-mediated degradation. In our mathematical model, [$DELLA_m$] and [DELLA] represent total DELLA mRNA and protein, respectively.

The only *GA2ox* family member to respond to gibberellin in our dataset was *GA2ox6*. The spatial expression profiles of *GA20ox2*, *GA3ox1*, *GID1a*, *RGA*, and *GAI* (but not *GA2ox6*) all overlap in the tip of the root, and therefore, a *GA2ox6* feedback loop is unlikely to interact directly with the rest of the network (18). Thus, we consider

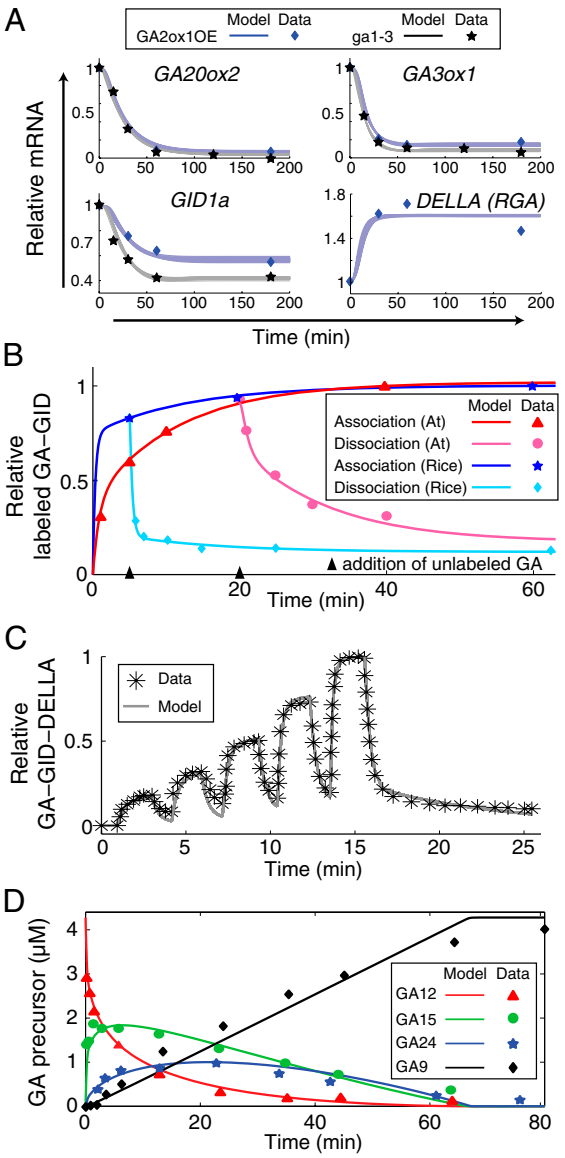

Fig. 2. Data and model fitting. (*A*) Transcriptional responses to 2 μM exogenous GA_4 (from time 0) in GA-deficient plants [*ga1–3* (2, 17) and GA2ox1OE (this work)] and corresponding fits of the reduced GA signaling model. (*B*) Labeled GA_4–GID1 after the addition of radiolabeled GA_4 (association), and for dissociation, labeled GA_4–GID1 after the addition of excess unlabeled GA_4 at 5 min for rice and 20 min for *Arabidopsis* (3, 22). Fits with the GA_4–GID1 binding model (Eqs. **1** and **2**) show excellent agreement. (*C*) Fits of the GA_4–GID1–DELLA binding model (Eqs. **3**–**5**) to data from ref. 25. Immobilized DELLA is periodically exposed to pulses of the GA_4–GID1 complex of increasing amplitude. (*D*) Fits of the in vitro biosynthesis model (Eq. **6**) to data from ref. 26. The initial substrate GA_{12} is converted by GA20ox to its final product GA_9 (Fig. 1).

GA2ox family members as constitutively active components of the network (which provide a constant rate of gibberellin deactivation), and we only consider gibberellin feedback regulation on *GID1*, *GA20ox*, *GA3ox*, and *DELLA* (Fig. 1, GA response). We find that this assumption is justified by our validation of the model (*Predictions and Validation*).

Parameterization of the Gibberellin Perception Model Reveals the Importance of a Conformational Change in GID1. Initial efforts to fit experimental data on GA_4–GID1 binding (3, 22) using simple association–dissociation kinetics (see Eq. **1**) were unsuccessful (*SI Appendix*, Fig. S1). This finding is largely because of the

appearance of two timescales in GA_4–GID1 binding kinetics (Fig. 2*B*): levels of GA_4–GID1 complex rapidly rise, after which their accumulation slows noticeably. However, GID1 [in rice (23) and *Arabidopsis* (24)] has an N-terminal strand that closes over the GA_4 binding pocket when the gibberellin is bound. This conformational change (closing the lid) allows DELLA to bind the GA_4–GID1 complex. Including reactions representing this conformational change (see Eqs. **1** and **2**), we obtain excellent agreement between the model and the association and dissociation experiments in rice (22) and *Arabidopsis* (3) (Fig. 2*B*). These experiments yield well-constrained parameter estimates for the binding of GA_4 to its receptor GID1 (in rice) or GID1a (in *Arabidopsis*) and the rates at which occupied GID1/GID1a opens and closes the lid (*SI Appendix*, Fig. S2*A* and Table S2). Our results indicate that, in rice, GA_4 can rapidly bind GID1, but the opening and closing of the GID1 lid is comparatively slow. For *Arabidopsis*, the timescales of GA_4–GID1a binding and the opening and closing of the GID1a lid are more similar.

The interaction between GID1 and DELLA proteins is thought to occur through the DELLA/TVHYNP motif (22, 24). Recently, the work by Hirano et al. (25) reported that, on GA_4–GID1 binding to this motif in the rice DELLA protein SLENDER RICE1 (SLR1), the GRAS domain of SLR1 can also interact with GID1. This last interaction is thought to have a stabilizing effect on the GA_4–GID1–DELLA complex and allow the DELLA to be targeted for degradation. Fig. 2*C* illustrates the excellent agreement between our model of GA_4–GID1–DELLA binding (see Eqs. **3** and **5**) and the time course experiments in ref. 25, in which immobilized DELLA is exposed to GA_4–GID1 pulses of increasing amplitude (*SI Appendix*). Parameter estimates seem to be well-constrained by the data (*SI Appendix*, Fig. S2*B*). In accordance with the experimental evidence, we find that the dissociation rate of the stable complex is noticeably smaller than the rate for the unstable complex.

Modeling Gibberellin Biosynthesis Reveals That Conversion of GA_{24} Is Rate-Limiting. Simulations from fitting our model of the gibberellin biosynthesis pathway (see Eq. **6**) to the in vitro GA20ox time course data in ref. 26 are summarized in Fig. 2*D*. The corresponding parameters are given in *SI Appendix*, Table S3. The penultimate step of the pathway, where GA_{24} is converted to GA_9 (with rate constant $k_{m_{24}}$), is predicted to be rate-limiting; all other conversion steps in the pathway are predicted to be relatively fast. This finding is consistent with the data, where GA_{15} and GA_{24} rise rapidly, but there is a lag before GA_9 begins to accumulate (Fig. 2*D*).

Integrating Gibberellin Perception and Response. To parameterize DELLA-mediated regulation of *GA20ox2*, *GA3ox1*, *GID1a*, and *DELLA* expression, we fit a reduced version of the gibberellin signaling model (*Materials and Methods*) to the transcriptomic data from *ga1–3* and GA2ox1OE plants that have low levels of endogenous GA_4. The model reduction is based on the expectation that, in such plants, the contribution of the gibberellin biosynthesis pathway is negligible. Fig. 2*A* shows an ensemble of best fits between the model and data (relative mRNA expression). The corresponding parameter sets are illustrated in *SI Appendix*, Fig. S4.

Our parameter estimates indicate that, in both plants, the initial levels of GA_4 are low and DELLA protein concentrations are high. This finding is consistent with the phenotypes of both *ga1–3* and GA2ox1OE plants, which have reduced size (8, 19, 27). Thus, the rates of transcription of the *GA20ox2*, *GA3ox1*, and *GID1a* mRNAs are predicted to be initially high. After exposing the plants to exogenous GA_4, the concentration of DELLA proteins decreases, leading to decreases in expression of *GA20ox2*, *GA3ox1*, and *GID1a*. *GID1a* mRNAs are not entirely depleted during the course of the experiments, whereas *GA20ox2* mRNAs become negligible. These differences in sensitivity are reflected in the model parameters by the concentration thresholds for DELLA-regulated transcriptional regulation (θs in Eqs. **9** and **10**). Estimates of the various mRNA decay rates (ψs in Eqs. **9** and **10**) indicate that *GA20ox2* and *GID1a* have similar decay rates, whereas the decay of *GA3ox1* is significantly faster. *DELLA* (*RGA*) mRNAs are predicted to have the fastest turnover rate overall.

Predictions and Validation. Because the *ga2ox quintuple* mutant knocks out all five *Arabidopsis* C_{19}-GA2ox (13), such plants have high intrinsic GA_4 levels, and hence, they respond weakly to the addition of exogenous GA_4 (13). However, treatment of plants with paclobutrazol (PAC) reduces GA_4 levels by inhibiting biosynthesis (28–30), and hence, PAC-treated plants are expected to respond more strongly to exogenous GA_4. Simulations of the full model using the parameters estimated above predict increasing magnitudes of target gene responses to exogenous GA_4, in the following order: *ga2ox quintuple* mutant, WT, *ga2ox quintuple* mutant + PAC, and WT + PAC (Fig. 3). Quantification of mRNA time courses for *GA20ox2*, *GA3ox1*, *GID1a*, and *RGA* in GA_4-treated plant roots agrees with this ordering and the predicted temporal dynamics (Fig. 3, *Insets*). Furthermore, both the model and experimental data show that *GA3ox1* transcript depletion is significantly faster than *GA20ox2* transcript depletion.

Roles of Transcriptional Feedback. The various feedback loops in the gibberellin signaling network may provide a mechanism for gibberellin homeostasis (31) and may also modulate the response to dynamic changes in GA_4, such as changes that might arise because of environmental variation or through transport of GA_4 from other tissues (15, 32). We consider the relevant response of the system to be the total concentration of DELLA protein. The work by Fu and Harberd (8) found the length of *ga1–3* roots to be 27% of WT, the length of *ga1–3 gai-t6* roots to be 35% of WT, and the length of *ga1–3 rga-24* roots to be 54% of WT. Because DELLA inhibits growth, this ordering implies a reverse ordering of DELLA concentration —consistent with this finding, *ga1–3* has low GA_4 and hence, high DELLA; we find that *GAI* and *RGA* account for 38% and 62%, respectively, of detectable *DELLA* mRNA expression in GA2ox1OE roots. Fig. 4*A* shows the predicted DELLA concentration in the four plant types (*ga1–3*, *ga1–3 gai-t6*, *ga1–3 rga-24*, and WT) with the expected ordering. Furthermore, these results set the range of DELLA concentrations (~1–5 nM) over which we expect to see physiologically relevant changes (such as in root growth). DELLA protein concentrations lower than 1 nM are unlikely to result in significantly longer roots, because gibberellin-treated WT roots that will have lower DELLA are of a similar length as untreated WT ones (13).

We now consider how DELLA protein steady states and dynamic responses change when regulated transcription of single or

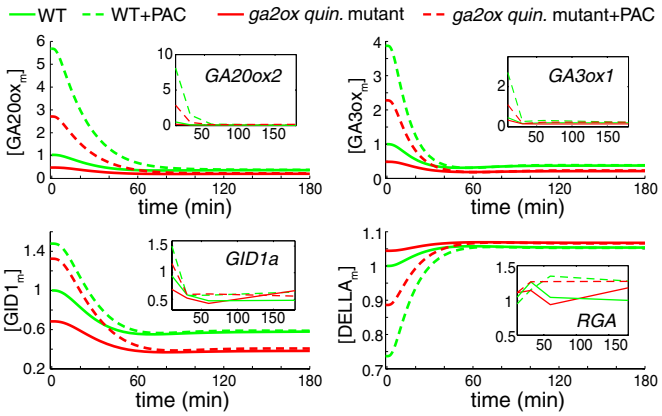

Fig. 3. Predicted dynamics in GA_4-treated roots for WT and *ga2ox quintuple* mutant in the presence and absence of PAC. *Insets* show corresponding RT-PCR data, showing good agreement with the model predictions.

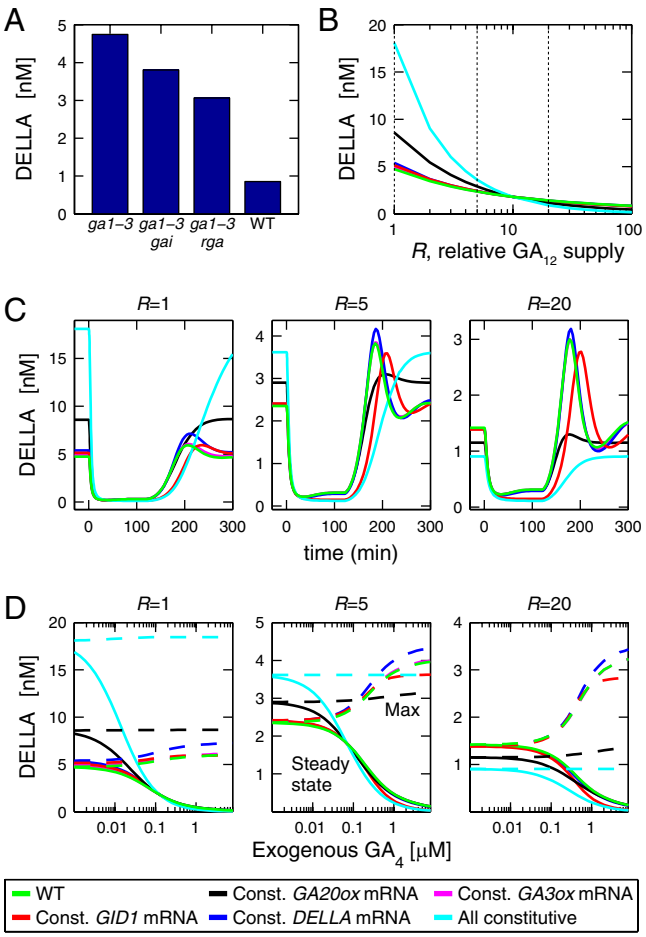

Fig. 4. (*A*) Predicted DELLA protein in *ga1–3, ga1–3 gai, ga1–3 rga*, and WT plants. (*B–D*) gibberellin signaling with different transcriptional feedbacks replaced by constitutive production. (*B*) Steady-state DELLA protein concentration as the relative gibberellin substrate supply, *R*, varies. *R* = 1 corresponds to *ga1–3* plants, and *R* = 100 corresponds to WT. Dotted lines indicate the values of *R* used in *C* and *D*. (*C*) DELLA protein response to a pulse of exogenous GA_4 (2 μM, *t* = 0–2 h) for three values of *R*. (*D*) Solid curves show the steady-state DELLA protein with exogenous GA_4. Dashed curves show the maximum DELLA protein in the overshoot after GA_4 removal.

multiple genes is replaced with constitutive transcription (with a constant transcription rate equal to the rate seen at steady state for a representative intermediate level of endogenous gibberellin, $\omega_{GA12} = 10\omega_{GA12}^{ga1-3}$). Fig. 4*B* shows that the WT steady-state DELLA protein concentration decreases with gibberellin substrate availability (ω_{GA12}), but with constitutive *GA20ox* mRNA, for low ω_{GA12}, DELLA protein is significantly higher than WT. This result is because high DELLA, through *GA20ox* feedback, would lead to an increase in GA_4 biosynthesis and hence, enhanced DELLA degradation. The other feedbacks have a weaker effect, but when all mRNAs are constitutive together, the net effect is greater than the sum of the parts. In particular, this synergy can be observed between *GA20ox* and *DELLA* feedbacks and between *GA20ox* and *GID1* feedbacks (*SI Appendix*, Fig. S6). Furthermore, these differences occur for DELLA concentrations relevant for root growth. In contrast, for high endogenous GA (high ω_{GA12}), the constitutive *GA20ox* mRNA gives DELLA levels below WT, but these levels are predicted to be too low to be physiologically significant.

We next consider the response to a pulse of exogenous GA_4 for three different levels of endogenous gibberellin. Fig. 4*C* shows that the initial response is quite robust to variations in feedback regulation, although the initial state, before the pulse, strongly differs (Fig. 4*B*). The *GID1* feedback loop gives a small degree of adaptation to the GA_4 stimulus (without this feedback, the DELLA protein concentration is lower than in the WT). Constitutive *GID1* mRNA also gives delayed recovery after the removal of exogenous GA_4. In addition, Fig. 4*C* shows that feedback in *GA20ox* transcription is mainly responsible for a DELLA overshoot that is seen when a GA_4 stimulus is removed (with constitutive *GA20ox* transcription, the overshoot is significantly smaller). These effects are increased in a synergistic manner when all feedbacks are constitutive (overshoots are completely eliminated and recovery is markedly slower).

We also characterize the response by considering a wide range of GA_4 doses. Fig. 4*D* shows that, at low GA_4 doses, the untreated steady state dominates the behavior—without *GA20ox* feedback, DELLA levels are elevated. At higher exogenous GA_4 concentrations, the various dose–response curves almost overlap, and DELLA protein levels are likely to be too small to be physiologically significant. Furthermore, the maximum DELLA protein concentration in the overshoot after removal of exogenous GA_4 is strongly dependent on the GA_4 dose and *GA20ox* feedback. Without feedback on *GA20ox* transcription, the maximum is barely above the untreated steady state (to which the system eventually returns), and therefore, the overshoot is almost eliminated.

Conclusions

Although many components of the gibberellin signaling network have been identified, little is known about how the various feedback loops (Fig. 1) interact to control responses to changes in gibberellin. To answer this question, we have developed a mathematical model of gibberellin signal transduction. The model is in good agreement with the available data, which ranges from ligand receptor binding kinetics to transcriptional responses to exogenous gibberellin (Fig. 2), and we tested the validity of the model using both chemical and genetic perturbations (Fig. 3). We found that the GA_4–GID1 complex undergoes slow conformational changes (lid opening and closing), an order of magnitude slower than the related complex dissociation rate and the same order of magnitude as the *GID1*, *DELLA*, *GA20ox*, and *GA3ox* mRNA turnover rates. The dominant feedback was in *GA20ox* mRNA, but this feedback is highly synergistic with *GID* and *DELLA* regulation. In particular, *GA20ox* feedback is important for determining the level of endogenous DELLA (Fig. 4*B*) and generating overshoots after pulses of exogenous GA_4 (Fig. 4 *C* and *D*). For exogenous GA_4 concentrations above about 0.1 μM, with the exception of the overshoots, the qualitative response is rather robust to perturbations in the various feedback loops.

It is important to note that the predicted role of *GA20ox* may depend on its translation rate, which sets its characteristic concentration level. For lower *GA20ox* translation rates, the role of *GA20ox* feedback is more pronounced, whereas for higher translation rates, this enzyme is more abundant. Therefore, feedback regulation has a weaker effect (*SI Appendix*, Fig. S7). Nevertheless, *GA20ox* regulation is still the main driver for an overshoot, and there is still strong synergy with feedbacks that have weak effects in isolation. *GA3ox* translation rates must be lowered 100-fold to see any noticeable differences caused by *GA3ox* regulation (*SI Appendix*, Fig. S8), but overall, we find that *GA3ox* feedback has very weak effects on gibberellin signaling. Crucially, the 10 best-fit parameter sets all give similar predictions (*SI Appendix*, Fig. S9).

Ultimately, it is hoped that this model will be extended to include the effects of cross-talk from other hormones (8) and environmental signals, such as the response to light. Moreover, the model has recently been embedded in a multiscale spatial model of root growth, which has been used to explore the interplay between gibberellin signaling and growth (33).

Materials and Methods

Mathematical Models. Here, we summarize our mathematical model of the GA signaling network (Fig. 1). The full model, a system of 21 coupled nonlinear ordinary differential equations with 42 parameters, is given as Systems Biology Markup Language (SBML) in Dataset S1.

Gibberellin perception. GA_4 binds reversibly to GID1; bound GID1 undergoes a conformational change, whereby its lid closes (at rate q) and opens (at rate p):

$$GID1^{o} + GA_4 \underset{l_d}{\overset{l_a}{\rightleftharpoons}} GID1^{o}.GA_4, \quad [1]$$

$$GID1^{o}.GA_4 \underset{p}{\overset{q}{\rightleftharpoons}} GID1^{c}.GA_4. \quad [2]$$

Superscripts o and c indicate that the lid is open and closed, respectively.

The interaction between the $GID1^{c}.GA_4$ complex and the DELLA protein SLR1 (found in rice) occurs through the DELLA/TVHYNP motif (23) or both this motif and the GRAS domain of the DELLA protein (25). The latter interaction is thought to be more stable and allow the DELLA to be tagged with ubiquitin, and hence, the interaction allow DELLA to be targeted for degradation:

$$GID1^{c}.GA_4 + DELLA \underset{u_{d_1}}{\overset{u_{a_1}}{\rightleftharpoons}} GID1^{c}.GA_4.DELLA_1, \quad [3]$$

$$GID1^{c}.GA_4.DELLA_1 \xrightarrow{u_m} GID1^{c}.GA_4 + DELLA^{*}, \quad [4]$$

$$GID1^{c}.GA_4 + DELLA \underset{u_{d_2}}{\overset{u_{a_2}}{\rightleftharpoons}} GID1^{c}.GA_4.DELLA_2. \quad [5]$$

Subscripts distinguish the two types of binding: 1 indicates the more stable binding, which mediates degradation of DELLA proteins, and 2 indicates the less stable form.

Gibberellin biosynthesis. The gibberellin precursor, GA_{12}, is assumed to be produced at a constant rate ω_{GA12}. GA_{12} is converted to GA_{15}, then to GA_{24}, and finally, to GA_9, and each time, it is facilitated by members of the GA20ox family of enzymes:

$$GA_X + GA20ox \underset{k_{d_X}}{\overset{k_{a_X}}{\rightleftharpoons}} GA_X.GA20ox \xrightarrow{k_{m_X}} GA_Y + GA20ox \text{ for } (X, Y) = \{(12, 15), (15, 24), (24, 9)\}. \quad [6]$$

In the final step of the biosynthesis pathway, GA3ox converts GA_9 to GA_4:

$$GA_9 + GA3ox \underset{k_{d_9}}{\overset{k_{a_9}}{\rightleftharpoons}} GA_9.GA3ox \xrightarrow{k_{m_9}} GA_4 + GA3ox. \quad [7]$$

As noted in the Introduction, GA2ox can deactivate GA_4 and its precursors (11). Experimental evidence (*Capturing gibberellin Network Topology*) indicates that, for root tips, GA2oxs are not feedback-regulated, and therefore, we model deactivation of the gibberellins by assuming that each GA is turned over at a constant rate μ_{GA}.

Exogenous GA4. GA_4 is a weak acid and can exist in protonated or anionic form. The protonated form can diffuse through the cell membrane, whereas diffusion of the anionic form is negligible. We assume that the rate of GA_4 transport across the cell membrane of a root is given by

$$P_{mem}\frac{S_{root}}{V_{root}}(A_1\omega_{GA4} - B_1 GA_4), \quad [8]$$

where ω_{GA4} is the externally applied concentration of GA_4, P_{mem} is the permeability of the membrane, S_{root} is the root surface area, V_{root} is the root volume, and A_1 and B_1 are the proportions of protonated GA_4 in the cell wall and cytoplasm, respectively (their estimated values are given in *SI Appendix, B.1 Exogenous GA4*).

Gibberellin-mediated gene regulation. We write $[X_m]$ for the concentration of an mRNA and $[X]$ for the corresponding protein. GA20ox, GA3ox and GID1 are up-regulated by DELLA protein, and therefore, the rate of mRNA transcription is an increasing function of [DELLA] that is balanced by degradation at a rate φ_X and normalized such that the maximum possible steady-state mRNA concentration is equal to one:

$$\frac{d[X_m]}{dt} = \varphi_X\left(\frac{[DELLA]}{[DELLA] + \theta_X} - [X_m]\right) \text{ for } X = \{GA20ox, GA3ox, GID1\}. \quad [9]$$

Transcription of DELLA mRNA is repressed by DELLA protein, and therefore, we use the equivalent decreasing form of transcription rate:

$$\frac{d[DELLA_m]}{dt} = \varphi_{DELLA}\left(\frac{\theta_{DELLA}}{[DELLA] + \theta_{DELLA}} - [DELLA_m]\right). \quad [10]$$

Because all mRNA data are relative, this normalization is the natural choice. In all cases, θ_X is the DELLA protein concentration for half-maximal transcription. We also assume that X_m is translated at a rate δ_X and that the gibberellin biosynthesis enzymes (GA20ox and GA3ox) and the gibberellin receptor (GID1) are degraded at a constant rate μ_X. DELLA proteins are turned over by the mechanism described in Eqs. **3–5**.

Plant Material and Treatments. *A. thaliana* Columbia-0 (Col-0) ecotype and *ga2ox quintuple* mutant (13) were used. Seeds were surface-sterilized and plated on one-half (0.5) Murashige Skoog (MS) and BactoAgar (Scientific Laboratory Supplies) 1% (wt/vol) solidified medium. Seedlings grew vertically in a growth chamber with constant conditions (24 °C and 150 μmol/m^2 per second), permitting roots to grow along the surface of the agar. The roots of 5-d-old seedlings were submerged in 0.5 MS liquid media with or without 0.1 μM PAC (an inhibitor of GA biosynthesis) (29) treatment as required. Two days later, 2 μM GA_4 was added to the liquid media, and material (whole roots) was collected after 0, 30, 60, and 180 min of GA_4 treatment. The GA2ox1OE line (19) was grown vertically on full-strength MS plates containing Gamborg B5 vitamins, 1% sucrose, pH 5.8, and 0.8% Gelrite under continuous light (22 °C and 150 μmol/m^2 per second). After 6 d, plants were placed with roots submerged in an acclimatization bath containing full-strength MS salts with Gamborg B5 vitamins (pH 5.8). After 24 h, plates were transferred to a treatment bath or control bath (±2 μM GA_4). Approximately 150 root tips were harvested into liquid nitrogen at 0, 30, 60, and 180 min after treatment.

RNA Isolation, Microarray Analysis, and Quantitative RT-PCR. Total RNA was extracted from GA2ox1OE root tips with on-column DNase treatment (RNeasy; Qiagen) and treated again with DNase in solution (Turbo DNA-Free Kit; Ambion). RNA was labeled and hybridized to the Affymetrix GeneChip *Arabidopsis* ATH1 Genome Array (NASC). For quantitative RT-PCR analysis, total RNA was extracted using the TRIzol reagent (Invitrogen) and the RNeasy Mini Kit (Qiagen). The first-strand cDNA was synthesized using the Transcriptor First Strand cDNA Synthesis Kit (Roche). Quantitative RT-PCR analysis was conducted using the following gene-specific primers: qGA20ox2-L (gaagcttgcaccaaacacg) and qGA20ox2-R (gcatccgctattagtgactcg) for AtGA20ox-2; qGA3ox1-L (tgccttccaaatctcaaacc) and qGA3ox1-R (accggtgagaaactcaatgtc) for AtGA3ox-1; qGID1a-L (gctgcgagcgatgaagtta) and qGID1a-R (ttgtaggctactttgaagttggatatt) for GID1A; qRGA-L (tacatcgacttcgacgggta) and qRGA-R (gttgtcgtcaccgtcgttc) for RGA; and qCTRL3-L (gaagtgtctcgacaaaggtcgt) and qCTRL3-R (ccttttggcacttctggtg) for At5G18800 used as control. PCR amplification reactions were prepared using the SensiMixSYBR kit (Bioline). Amplifications were monitored in real time with the LightCycler480 II (Roche). Experiments were performed in duplicate from RNA of root tissue. Amplification of AT5G18800 (NADH–ubiquinone oxidoreductase 19-kDa subunit) served as the control. Quantitative RT-PCR was performed two or three times, and results were comparable in all experiments.

Parameter Estimation and Experimental Data. For the parameter estimation problems described below, we used the Matlab Optimization toolbox to minimize the error between the data and model simulations (*SI Appendix*).

In vitro perception pathway. For GID1–GA_4 binding, we fit the parameters of a submodel corresponding to Eqs. **1** and **2** using the association and dissociation time course data in refs. 3 and 22. The total levels of GA_4 and GID1 are constant, and these parameters were obtained from refs. 3 and 22. For DELLA binding to GA_4–GID1 (Eqs. **3–5**), we fit the relevant submodel to the association and dissociation data in ref. 25. The total concentrations of GID1 and GA_4 used are provided (25), and from these concentrations, we estimate the total concentration of GA_4–GID1. The total concentration of DELLA used is not provided, and we treat this concentration as a parameter to be estimated.

In vitro biosynthesis. In the work by Appleford et al. (26), GA20ox1 (from wheat) was incubated with GA_{12}, and the concentrations of GA_{12}, GA_{15}, GA_{24}, and GA_9 were measured. To estimate the association, dissociation, and modification rates for the three steps of the GA20ox-catalyzed reaction, we fit our model of this part of the GA biosynthesis pathway (Fig. 1 and Eq. **6**) to the time series data in ref. 26.

In vivo transcriptional response. We use two published datasets comprising changes in the relative levels of GID1, GA20ox, and GA3ox mRNA after treatment of *ga1–3* plants with 2 μM GA_4 (2, 17). We generated complementary data using transgenic GA2ox1OE *Arabidopsis* roots. Because both *ga1–3* and GA2ox1OE plants have low levels of endogenous GA_4, effects from gibberellin biosynthesis feedback (through the regulation of GA20ox and GA3ox genes) should be negligible during treatment with exogenous GA_4. We exploit this finding to

derive a simplified model in which the equations governing biosynthesis decouple from the system. Because we have data on the dynamics of gibberellin biosynthesis mRNAs, we include the equations governing their dynamics in the model. We then used the parameters already obtained for gibberellin perception and estimated the parameters for transcriptional regulation of GA-responsive genes by fitting the reduced model to the data from *ga1–3* and GA2ox1OE plants. We consider the data for *RGA* as representative of the total concentration of regulated *DELLA* family members (*SI Appendix*, Fig. S3).

Generating Predictions for the Full System. We use the best-fit parameter sets obtained from the gibberellin biosynthesis, perception, and transcriptomic data. GA20ox and GA3ox translation and protein decay rates could not be estimated because of the decoupling of biosynthesis from the transcriptional response. We assume that GA20ox and GA3ox decay occurs at a similar rate to GID1, and we choose translation rates to give nanomolar concentrations of these enzymes. In addition, we assume that the parameters for the final step of GA_4 biosynthesis (GA3ox-mediated conversion of GA_9 to GA_4) (Eq. **7**) are similar to those parameters for the GA20ox-mediated conversion of GA_{15} to GA_{24}. These two conversion steps have similar reported values for their Michaelis constants [1–1.5 μM for GA3ox (34–36) and 0.37 μM for GA20ox (26)].

We define the relative GA_{12} supply as $R = \omega_{GA12}/\omega_{GA12}^{ga1-3}$, where ω_{GA12}^{ga1-3} is the predicted rate of GA_{12} synthesis in *ga1–3* roots. Thus, $R = 1$ corresponds to *ga1–3* plants, and we model WT plants by setting $R = 100$. This scaling gives a WT endogenous GA_4 concentration of about 0.1 μM, ∼10 times greater than in *ga1–3* plants. To model the effect of 0.1 μM PAC, we set $R = 1$, and for the ga2ox quintuple mutant, we reduce the decay rate of GA_4 and its precursors: $\mu_{GA} = 0.4\mu_{GA}^{ga1-3}$ (40% of the decay rate predicted for *ga1–3* roots). To model mutations in *GAI* and *RGA*, we assume that loss of these genes corresponds to an equivalent reduction in the DELLA translation rate (because mRNAs are all normalized). *SI Appendix* includes the full parameter set (*SI Appendix*, Table S3) and shows that simulations of the full model when endogenous gibberellin is low are indeed close to those simulations of the reduced model (*SI Appendix*, Fig. S5).

ACKNOWLEDGMENTS. This work was conducted in the Centre for Plant Integrative Biology, University of Nottingham, which is jointly funded by Biotechnology and Biological Sciences Research Council/Engineering and Physical Sciences Research Council Grant BB/D0196131 as part of their Systems Biology Initiative. Rothamsted Research receives grant-aided support from the Biotechnology and Biological Sciences Research Council of the United Kingdom.

1. Fleet CM, Sun TP (2005) A DELLAcate balance: The role of gibberellin in plant morphogenesis. *Curr Opin Plant Biol* 8:77–85.
2. Griffiths J, et al. (2006) Genetic characterization and functional analysis of the GID1 gibberellin receptors in *Arabidopsis*. *Plant Cell* 18:3399–3414.
3. Nakajima M, et al. (2006) Identification and characterization of *Arabidopsis* gibberellin receptors. *Plant J* 46:880–889.
4. Willige BC, et al. (2007) The DELLA domain of GA INSENSITIVE mediates the interaction with the GA INSENSITIVE DWARF1A gibberellin receptor of Arabidopsis. *Plant Cell* 19:1209–1220.
5. Dill A, Thomas SG, Hu J, Steber CM, Sun TP (2004) The *Arabidopsis* F-box protein SLEEPY1 targets gibberellin signaling repressors for gibberellin-induced degradation. *Plant Cell* 16:1392–1405.
6. McGinnis KM, et al. (2003) The Arabidopsis *SLEEPY1* gene encodes a putative F-box subunit of an SCF E3 ubiquitin ligase. *Plant Cell* 15:1120–1130.
7. Dill A, Sun T (2001) Synergistic derepression of gibberellin signaling by removing RGA and GAI function in *Arabidopsis thaliana*. *Genetics* 159:777–785.
8. Fu X, Harberd NP (2003) Auxin promotes *Arabidopsis* root growth by modulating gibberellin response. *Nature* 421:740–743.
9. King KE, Moritz T, Harberd NP (2001) Gibberellins are not required for normal stem growth in *Arabidopsis thaliana* in the absence of GAI and RGA. *Genetics* 159:767–776.
10. Richards DE, King KE, Ait-Ali T, Harberd NP (2001) How gibberellin regulates plant growth and development: A molecular genetic analysis of gibberellin signaling. *Annu Rev Plant Physiol Plant Mol Biol* 52:67–88.
11. Hedden P, Phillips AL (2000) Gibberellin metabolism: New insights revealed by the genes. *Trends Plant Sci* 5:523–530.
12. Fleet CM, et al. (2003) Overexpression of AtCPS and AtKS in Arabidopsis confers increased ent-kaurene production but no increase in bioactive gibberellins. *Plant Physiol* 132:830–839.
13. Rieu I, et al. (2008) Genetic analysis reveals that C_{19}-GA 2-oxidation is a major gibberellin inactivation pathway in Arabidopsis. *Plant Cell* 20:2420–2436.
14. Thomas SG, Phillips AL, Hedden P (1999) Molecular cloning and functional expression of gibberellin 2- oxidases, multifunctional enzymes involved in gibberellin deactivation. *Proc Natl Acad Sci USA* 96:4698–4703.
15. Yamaguchi S (2008) Gibberellin metabolism and its regulation. *Annu Rev Plant Biol* 59:225–251.
16. Cao D, Cheng H, Wu W, Soo HM, Peng J (2006) Gibberellin mobilizes distinct DELLA-dependent transcriptomes to regulate seed germination and floral development in *Arabidopsis*. *Plant Physiol* 142:509–525.
17. Zentella R, et al. (2007) Global analysis of della direct targets in early gibberellin signaling in Arabidopsis. *Plant Cell* 19:3037–3057.
18. Dugardeyn J, Vandenbussche F, Van Der Straeten D (2008) To grow or not to grow: What can we learn on ethylene-gibberellin cross-talk by in silico gene expression analysis? *J Exp Bot* 59:1–16.
19. Rieu I, et al. (2008) The gibberellin biosynthetic genes AtGA20ox1 and AtGA20ox2 act, partially redundantly, to promote growth and development throughout the Arabidopsis life cycle. *Plant J* 53:488–504.
20. Silverstone AL, Ciampaglio CN, Sun T (1998) The *Arabidopsis* RGA gene encodes a transcriptional regulator repressing the gibberellin signal transduction pathway. *Plant Cell* 10:155–169.
21. Ogawa M, Kusano T, Katsumi M, Sano H (2000) Rice gibberellin-insensitive gene homolog, OsGAI, encodes a nuclear-localized protein capable of gene activation at transcriptional level. *Gene* 245:21–29.
22. Ueguchi-Tanaka M, et al. (2005) *GIBBERELLIN INSENSITIVE DWARF1* encodes a soluble receptor for gibberellin. *Nature* 437:693–698.
23. Ueguchi-Tanaka M, et al. (2007) Molecular interactions of a soluble gibberellin receptor, GID1, with a rice DELLA protein, SLR1, and gibberellin. *Plant Cell* 19:2140–2155.
24. Murase K, Hirano Y, Sun TP, Hakoshima T (2008) Gibberellin-induced DELLA recognition by the gibberellin receptor GID1. *Nature* 456:459–463.
25. Hirano K, et al. (2010) Characterization of the molecular mechanism underlying gibberellin perception complex formation in rice. *Plant Cell* 22:2680–2696.
26. Appleford NE, et al. (2006) Function and transcript analysis of gibberellin-biosynthetic enzymes in wheat. *Planta* 223:568–582.
27. Hedden P, Phillips AL (2000) Manipulation of hormone biosynthetic genes in transgenic plants. *Curr Opin Biotechnol* 11:130–137.
28. Hedden P, Graebe JE (1985) Inhibition of gibberellin biosynthesis by paclobutrazol in cell-free homogenates of *Cucurbita-maxima* endosperm and *Malus pumila* embryos. *J Plant Growth Regul* 4:111–122.
29. Olszewski N, Sun TP, Gubler F (2002) Gibberellin signaling: Biosynthesis, catabolism, and response pathways. *Plant Cell* 14(Suppl):S61–S80.
30. Rademacher W (2000) Growth retardants: Effects on gibberellin biosynthesis and other metabolic pathways. *Annu Rev Plant Physiol Plant Mol Biol* 51:501–531.
31. Gallego-Giraldo L, et al. (2008) Gibberellin homeostasis in tobacco is regulated by gibberellin metabolism genes with different gibberellin sensitivity. *Plant Cell Physiol* 49:679–690.
32. Harberd NP, Belfield E, Yasumura Y (2009) The angiosperm gibberellin-GID1-DELLA growth regulatory mechanism: How an "inhibitor of an inhibitor" enables flexible response to fluctuating environments. *Plant Cell* 21:1328–1339.
33. Band LR, et al. (2012) Growth-induced hormone dilution can explain the dynamics of plant root cell elongation. *Proc Natl Acad Sci USA* 109:7577–7582.
34. Martin DN, Proebsting WM, Hedden P (1997) Mendel's dwarfing gene: cDNAs from the Le alleles and function of the expressed proteins. *Proc Natl Acad Sci USA* 94: 8907–8911.
35. Williams J, Phillips AL, Gaskin P, Hedden P (1998) Function and substrate specificity of the gibberellin 3β-hydroxylase encoded by the *Arabidopsis GA4* gene. *Plant Physiol* 117:559–563.
36. Zhou R, Yu M, Pharis RP (2004) 16,17-dihydro gibberellin A5 competitively inhibits a recombinant *Arabidopsis* GA 3beta-hydroxylase encoded by the *GA4* gene. *Plant Physiol* 135:1000–1007.